Covariance Profiling for an Adaptive Kalman Filter to Suppress Sensor Quantization Effects

Author/Contributor:
Luong-Van, Daniel; Tordon, Michal J; Katupitiya, Jayantha

Publication details:
Proceedings of the 43rd IEEE Conference on Decision and Control
pp. 2680-2685
0-7803-8683-3 (ISBN)

Event details:
43rd IEEE Conference on Decision and Control
Atlantis, Paradise Island, Bahamas

Publication Date:
2004

DOI:
https://doi.org/10.26190/unsworks/87

Covariance Profiling for an Adaptive Kalman Filter to Suppress Sensor Quantization Effects

Daniel Luong-Van, Michal J. Tordon and Jayantha Katupitiya
School of Mechanical and Manufacturing Engineering
The University of New South Wales
Sydney NSW 2052, Australia
j.katupitiya@unsw.edu.au

***Abstract*— This paper presents a generic approach to model the noise covariance associated with discrete sensors such as incremental encoders and low resolution analog to digital converters. The covariance is then used in an adaptive Kalman Filter that selectively and appropriately carries out measurement updates. The temporal as well as system state measurements are used to predict the quantization error of the measurement signal. The effectiveness of the method is demonstrated by applying the technique to incremental encoders of varying resolutions. Simulation of an example system with varying encoder resolutions is presented to show the performance of the new filter. Results show that the new adaptive filter produces more accurate results while requiring a lower resolution encoder than a similarly designed conventional Kalman filter, especially at low velocities.**

I. Introduction

Quantization is an inherent feature in digitally controlled systems. For analog sensors, quantization occurs at the analog to digital converter. For discrete sensors such as incremental encoders, quantization occurs at the sensor itself. For estimators that attempt to determine states that have a derivative component of the sensed signal, the effects of quantization are detrimental. An example situation is the implementation of a sliding mode controller in which the only sensor is an incremental encoder. The sensed position may not be 100% accurate at the sampling instances. Worse than that is the estimated velocity, be it through differentiation or through an estimator employing a system model. If the sliding surface is a function of the estimated velocity, the behavior of the sliding mode controller becomes erratic. This paper presents a solution to this problem by implementing a covariance profiling function that is suitable for the sensor in question. Its success is demonstrated by implementing the method in a LQG type servo controller where the position is sensed using an encoder.

Incremental encoders are a prominent means for measuring relative displacement in control applications. They produce a predictable pattern of highly colored noise superimposed on their output. A simplified model of noise, based on the temporal information of the edge triggering, and the estimated velocity, is used to profile the measurement covariance error. Approaches to model quadrature encoder irregularities have lead to detailed models of encoder nonideality such as those found in [1] and [2], the latter compensating these via Kalman filtering for an analog quadrature encoder. In Kalman filtering, the measurement bandwidth is determined by the Kalman gain. The Kalman gain is dependent on the measurement noise covariance so by modifying the covariance, the filter weighting between measured and estimated states can be controlled [3]. It is important for the measurement covariance to be appropriately selected to allow for the filter to make appropriate measurement updates.

When a system moves within a quanta, the feedback signal is essentially ineffective as it is unable to observe any motion changes that fall within it. Measurements that can be detected as within a quanta are named *untrusted* measurements. As feedback is ineffective in this region it is proposed that the system should be controlled in open-loop. This is done by selecting a small Kalman gain which will bias the measurements toward the estimated state, ignoring the measurement update.

When a change in the sensed signal has been detected, the algorithm takes it as a *trusted* measurement, albeit though it may not be 100% accurate. A model of the covariance of the trusted measurements is based on a function of current estimated state, transducer accuracy and quantization edge triggering. It is assumed that the trusted values are bounded by a function of velocity, and inside the bounded range have a Gaussian noise distribution [4]. These trusted measurements will have a covariance considerably smaller than the untrusted values at low velocities. This increases the Kalman gain of the filter, and therefore allows for more accurate measurement updates when trusted readings are available, and to avoid inaccurate measurement updates at other times.

This new adaptive Kalman filter configuration allows for similar levels of noise rejection in comparison to the implementation of a traditional non adaptive filter. The improvement in state estimation may allow for the use of lower resolution measurement devices in certain classes of control problems.

II. Edge Level Based State Measurement

The basis behind the ideas in this paper is that there is additional information present in quantized signals that have high repeatability. Traditionally this information is ignored. Typically only the signal magnitude is used, but if the sampling rate is considerably higher than the rate at which the system transitions between quantized levels, there is also information about the error of the measured value that can be extracted. Estimating higher order states such as velocity are particularly difficult with high sampling rates or low velocities with the presence of quantization, using standard estimation techniques [5] [6] [7]. By using the temporal information of the quantized signal, the accuracy of the estimates may be improved.

With the assumption of an infinite sampling rate and a perfectly quantized signal, at the edge level transition, the signal magnitude would be known with certainty. Studies show that optical encoders have a high repeatability, triggering with a 3-5% error of the actual edge [5]. This means that their optical repeatability is 20-30 times higher than the count output accuracy. Analog comparators can show even higher repeatability. For the basic analysis that follows, it is assumed that the triggering error is negligible in comparison to the measured signal.

Fig. 1 shows a continuous signal that has been sampled and quantized. Trusted values occur when the measured quantized-value generates a positive or negative edge, indicating a change between samples. This leads to the phrase 'edge level based state measurement', these *trusted* values are indicated as plain dots. If no change occurs between samples, the reading is deemed *untrusted*, these values are circled. As the system is moving, the trusted values can deviate from the actual values, leading to the error shown in the figure.

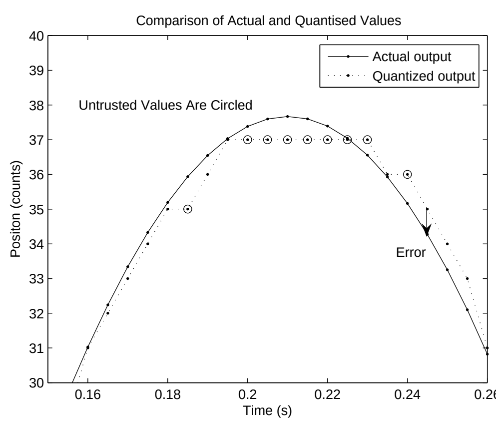

Fig. 1. Quantizing effects showing trusted and untrusted values

Distinguishing between the trusted and untrusted values, and modeling the predicted error in each case, is the basis for the proposed adaptive Kalman filter.

III. Covariance Profiling of Measurement Noise

To estimate the amount of quantization error present in the trusted values, the input signal rate of the change is needed. If a direct measurement is available, for instance from a tachometer, it can be used otherwise it must be estimated from the known system states. As the system has a fixed sampling rate, it is possible to bound the maximum error as a function of velocity. As the transducer measurement operation occurs almost instantaneously compared to the sampling interval, the maximum quantization has an upper bound of one quantized interval q. Fig. 2 shows the relation between velocity $\dot{\theta}$, and maximum error e_{max}. The maximum trusted-value quantization-error for a given velocity happens when the sampling occurs just before a quantized interval is traversed, while the minimum occurs when the sampling and quantized interval traversal times coincide. As the time at which the quantized level changes and the sampling instance are uncorrelated, it is assumed that this error has a Gaussian distribution between $0 \leftrightarrow e_{max}$ giving the expected error (2).

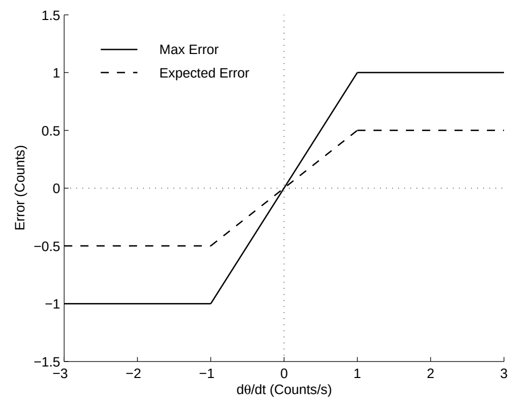

Fig. 2. Quantizing errors showing maximum and expected values

Maximum Quantization Error: [10]

$$e_{max}(\dot{\theta}) = \begin{cases} 1 & \dot{\theta}T_s > 1 \\ -1 & \dot{\theta}T_s < -1 \\ \dot{\theta}T_s & \text{otherwise} \end{cases} \quad (1)$$

$$\begin{aligned} e_{max} &= \text{Maximum quantization error} \\ T_s &= \text{Sampling rate} \\ \dot{\theta} &= \text{Encoder velocity} \end{aligned}$$

Expected Quantization Error:

$$E\{e\} = \frac{1}{2}e_{max} \quad (2)$$

As the trusted value error is a uniform probability distribution, it is rectangular in shape. The width being $T_s\dot{\theta}$ and the height $\frac{1}{\dot{\theta}T_s}$. The slower the velocity of the measured state, the more concentrated the distribution, this indicates that the lower the velocity, or the higher the sampling rate, the more precise the trusted value.

For a continuous process, its covariance is defined as in (3) [8]. The trusted measurement error has a mean $m_x(t) = \frac{\dot{\theta}T_s}{2}$ and a uniform probability distribution $f_x(x;t) = \frac{1}{\dot{\theta}T_s}$ with the assumption that $\dot{\theta}$ is constant. Calculating the covariance of the trusted value error as a function of velocity $\dot{\theta}$ with a fixed sampling rate T_s gives the relationship (4).

$$\begin{aligned}\Xi &= E\left[\{x(t)-m_x(t)\}\{x(t)-m_x(t)\}^T\right] \\ &= \int_{-\infty}^{\infty}\{x(t)-m_x(t)\}\{x(t)-m_x(t)\}^T \\ &\qquad f_x(x;t)dx \qquad (3)\end{aligned}$$

$$\begin{aligned}E[\,] &= \text{Expected value operator} \\ x(t) &= \text{Random sequence} \\ m_x(t) &= \text{Mean value of } x(t) \\ f_x(x;t) &= \text{Probability distribution function of } x(t)\end{aligned}$$

$$\begin{aligned}\Xi &= \int_0^{\dot{\theta}T_s}\left(x^2 - x\dot{\theta}T_s + \frac{(\dot{\theta}T_s)^2}{4}\right)\frac{1}{\dot{\theta}T_s}dx \\ &= \frac{1}{12}\left(\dot{\theta}T_s\right)^2 \qquad (4)\end{aligned}$$

Due to the bounding of the maximum quantized trusted error to ± 1 quantum, the measurement covariance R_t has a saturation function (5) [10]. The saturated value of covariance is in agreement with [4] which is the standard analytical value for quantization noise. As the system has a fixed sampling rate T_s, R_t is only a function of velocity $\dot{\theta}$. Of interest is the area $\left|\dot{\theta}T_s\right| < q$, in this region it is possible to extract more accurate system measurements, and therefore state estimates.

$$R_t(\dot{\theta}) = \begin{cases} \frac{1}{12}q^2 & \left|\dot{\theta}T_s\right| > q \\ \frac{1}{12}(\dot{\theta}T_s)^2 & \text{otherwise} \end{cases} \qquad (5)$$

$$\begin{aligned}R_t &= \text{Trusted measurement covariance} \\ q &= \text{Smallest quantized level}\end{aligned}$$

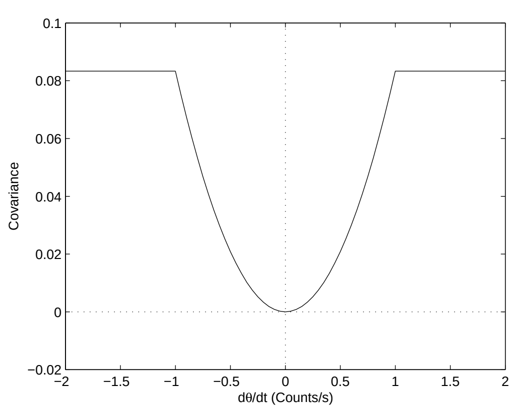

Fig. 3. Normalized covariance shape

IV. Modified Kalman Filter

The following section describes the modification of a standard Kalman filter to incorporate both trusted and untrusted measurement readings. It assumes the measured system to be linear time-invariant until the quantization function at the measurement y_k. All notation is as described in [9], with $(-)$ to indicate an estimate before measurement update and $(+)$ after the measurement update. As the main issue is focused on measurement noise, plant noise will not be discussed and is implemented as per standard convention.

The predicted error covariance and state estimates are updated via the following measurement update equations, where $\hat{x}_k(-)$ is the state estimate and $P_k(-)$ is the error covariance prior to measurement update.

$$\begin{aligned}\hat{x}_k(+) &= \hat{x}_k(-) + \bar{K}_k\left[y_k - H\hat{x}_k(-)\right] \qquad (6) \\ P_k(+) &= \left[I - \bar{K}_k H_k\right]P_k(-) \\ \bar{K}_k &= P(-)H^T\left[HP_k(-)H^T + R_k\right]^{-1} \qquad (7)\end{aligned}$$

The standard Kalman filter uses a non time-varying value of R while the new adaptive filter allows for this value to change as a function of both predicted velocity and encoder edge level state (8)(9) [10].

$$\dot{\theta} = H_{vel}\hat{x}_k(-) \qquad (8)$$

$$R_k = \begin{cases} R_t & \text{trusted} = 1 \\ R_u & \text{trusted} = 0 \end{cases} \qquad (9)$$

To select the scalar quantity of the measured velocity, H_{vel} is applied to the to the predicted state estimate $\hat{x}_k(-)$. R_t is the trusted covariance (5) and R_u is set to an arbitrary large value. By setting $R_u \approx 5\times 10^5$, $\bar{K} \to 0$ effectively ignoring the measurement update, which moves the estimator to strongly bias its open loop estimate $\hat{x}_k(-)$ during untrusted measurements.

The Kalman filter is designed for noise with a zero mean. As (2) shows the measurement noise to have a bias in the sign of velocity, with a bounding of ± 1 quantum. This bias should be corrected for a favorable application of the Kalman filter. It is proposed that to achieve a zero mean, y_k is updated via (10).

$$y_k^{'} = y_k + E[e] \qquad (10)$$

The final filter is created by modifying (6) and (7) with the substitution of R and y with (9) and (10). This new Kalman filter now integrates trusted and untrusted measurement and has measurement noise that is zero mean and uniformly distributed.

V. Simulation Results

A servo motor simulation was performed to investigate the quantization filtering performance of the modified Kalman filter. A simple LQG position controller design was implemented. As interest only lies in how accurately the filter estimates system state, further information on

TABLE I

STANDARD FILTER MEASUREMENT NOISE COVARIANCE

Counts per rev	R
4096	0.0833
2048	0.3333
1024	1.3333
512	5.3333

controller design has been omitted. A step and sine wave command input of various frequencies was used to show estimator performance over a range of different velocities (Fig. 4). The position of the shaft was sampled using a quantization function simulating an encoder of 4096, 2048, 1024 and 512 count per revolution to investigate the effect of various magnitudes of quantization. The final results have been normalized to the 4096 CPR encoder so that meaningful comparison can be made. The Kalman filter's system equations had a $+10\%$ time constant error introduced as a modeling inaccuracy.

To compare the performance of the new filter, a reference Kalman filter was designed using [4], $R = \frac{1}{12}q^2$ as the measurement noise covariance. The values for the different quantization levels are in Table I. The measurement updates were performed with the direct measurement of y, no unbiasing function was applied.

The system model used the following values:

$$\Phi = \begin{bmatrix} 1.0000 & 0.0049 \\ 0 & 0.9753 \end{bmatrix}$$
$$\Gamma = \begin{bmatrix} 0.0036 \\ 1.4339 \end{bmatrix}$$
$$H = \begin{bmatrix} 1 & 0 \end{bmatrix}$$
$$T_s = 0.005$$

With a full state feedback controller with the following values.

$$u_k = -K\hat{x}_k(+) + \bar{N}r$$

with:

$$K = \begin{bmatrix} 1.4205 & 0.1200 \end{bmatrix}$$
$$\bar{N} = 1.4205$$

where:

u_k = Control output

K = State feedback matrix

$\bar{N}$ = Reference gain

r = Reference input

To show the effectiveness of the trusted measurement error function $E[e]$, state measurement error values from the normal trusted y_k and the unbiased trusted $y_k^{'}$ values were plotted while all untrusted values were omitted (Fig. 5a). Fig. 5b shows a zoomed in section from the last sine wave period for a clearer indication of the effects of unbiasing

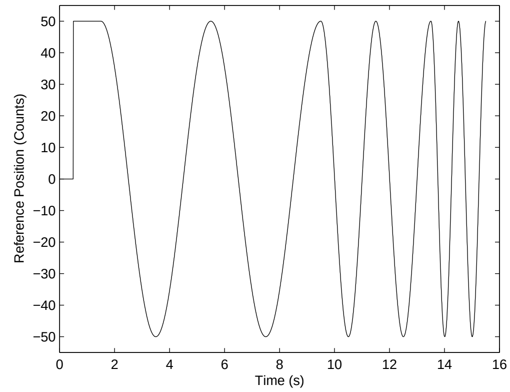

Fig. 4. Position command signal

the y measurement. As can be seen the unbiased error is much closer to a 0 mean, indicating the validity of (2).

To allow for comparison between the performance of the new adaptive filter to the standard Kalman filter, the feedback controller used the exact state vector x_k. This allowed for the estimators to be directly compared as they had the same state trajectory to predict. The position measurement was passed through a quantizing function to simulate an encoder. Each filter was run concurrently and the estimation error was defined as the difference between the actual state x_k and the filter estimate $\hat{x}_k(+)$. Fig. 6 shows the position errors for encoder resolutions of 2048 and 512 counts per revolution (CPR). As can be seen, the standard filter's positional noise is highly biased with the direction of velocity, while the new filter has near zero mean error. The adaptive filter more accurately tracks the position, even with a much reduced quantization resolution. Of interest is the steady state error on the initial step. This is due to the error introduced in the estimator system model. Regardless of estimator, it is impossible to get a final accuracy higher than the encoder output unless a perfect system model exists.

Fig. 7 shows the velocity error. As can be seen the new adaptive filter very effectively removes quantization effects for low velocities. As the velocity of the input signal increases, the error of both standard and adaptive estimators increase, and at high velocities the errors approach each other. The reason for this is that $\left|\dot{\theta}T_s\right|$ approaches q leading to both systems having the same amount of measurement noise covariance. As the measurement error bias of the standard encoder is roughly constant for a given velocity, this does not effect the estimated velocity, so the unbiasing function $y_k^{'}$ does not advantage the new filter. For low velocities the new filter clearly outperforms the traditional design while at high velocities it matches the maximum error but with less randomness.

A complete summary of the simulation is in Table II. This presents the inaccuracy of the estimator as a mean squared error to allow for easy comparison. The columns

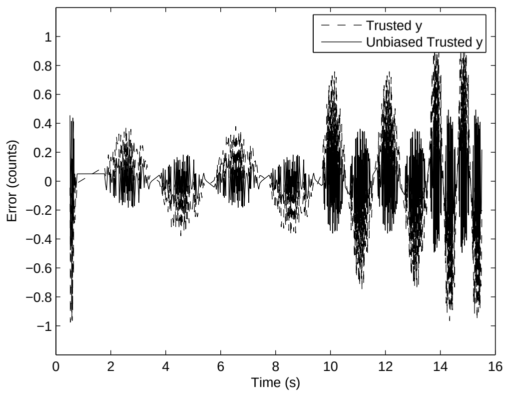

(a)

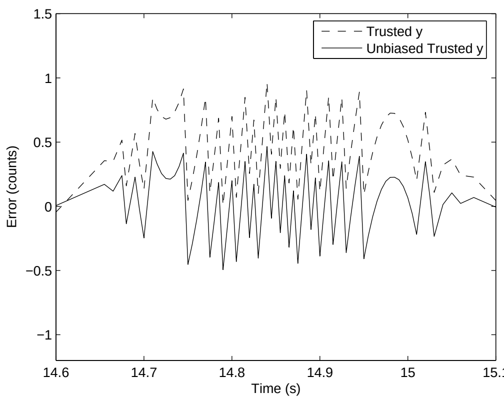

(b)

Fig. 5. a) Error comparison b) Zoom of error comparison

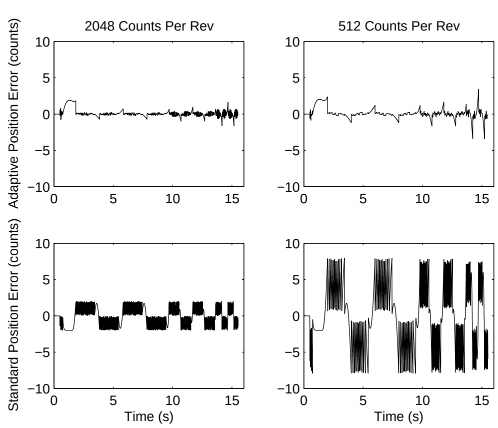

Fig. 6. Position error

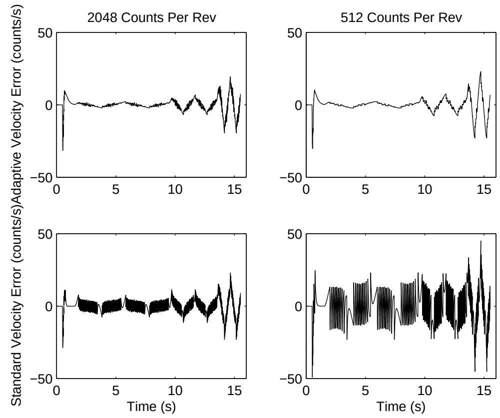

Fig. 7. Velocity error

TABLE II

ESTIMATOR MEAN SQUARE ERROR

4096 CPR	0.25*Hz*	0.5*Hz*	1.0*Hz*
Conv pos	0.5069	0.5045	0.5342
New pos	0.1340	0.1759	0.2364
Conv vel	1.2622	2.4305	7.3049
New vel	0.8264	2.6608	8.1144
2048 CPR			
Conv pos	1.0399	0.9703	1.0329
New pos	0.1906	0.2028	0.3470
Conv vel	2.2981	**3.2503**	8.0420
New vel	0.9181	2.8266	8.3307
1024 CPR			
Conv pos	1.8753	1.7972	1.9612
New pos	0.2322	0.2541	0.4003
Conv vel	4.1555	5.0823	9.9972
New vel	0.9697	2.8709	9.3334
512 CPR			
Conv pos	3.5312	3.5297	3.9654
New pos	0.3120	0.3080	0.6848
Conv vel	7.6090	8.9383	13.4968
New vel	1.0174	**3.1759**	10.3636

of the table are the different sinusoid frequencies to show the effect of the system velocity on the estimation error. The rows show the effect of the encoder resolution (CPR) and the filter used. As can be seen the position error is much improved with the new filter regardless of velocity or encoder resolution. Also apparent is the fact that at low to medium velocities, the new filter's velocity estimation is far more accurate. For velocity estimation with $\left|\dot{\theta}T_s\right| < 0.75q$ the new filter with a 512 CPR encoder performs similarly to that of a conventional estimator of 2048 counts, these values have been marked bold in the table.

VI. CONCLUSION

By adaptively profiling covariance depending on system state and quantization level edge-detection, the newly proposed Kalman filter effectively removes a significant amount of quantization noise. The method presented is based on the proposition that a quantized sensor has a lower level of uncertainty at the instance when it changes state, to when it is within a quantum. This property allows for a simple but effective method of improving state estimation.

The main application of this new filter is in allowing lower resolution discrete sensors to be used than would otherwise be necessary for the estimation of higher order states. There is no claim that final positional accuracy can be any higher than the quantization level. In the presented servo example, the new filter required 4 times less resolution to produce comparable results to the standard filter.

REFERENCES

[1] Kavanagh, R.C. and Murphy, J.M.D., ”The Effects of Quantization Noise and Sensor Nonideality on Digital Differentiator-based Rate Measurement”, *IEEE Transactions on Instrumentation and Measurement*, vol. 47, no. 6, 1998, pp 1497-1463.

[2] S. Venema and B. Hannaford, ”Kalman Filter Based Calibration of Precision Motion Control”, *Proceedings of the IEEE International Conference on Intelligent Robots and Systems*, vol. 2, no. 5-9, 1995, pp 224-229.

[3] Efe, M., Bather, J.A. and Atherton, D.P., ”An Adaptive Kalman Filter With Sequential Rescaling of Process Noise”, *Proceedings of the American Control Conference*, 1999, pp 3913-3917.

[4] Gene F. Franklin, G. F., Michael L. Workman and Dave Powell, *Digital Control of Dynamic Systems*, Addison-Wesley Longman Publishing Co., 1997, pp 434.

[5] Rull, J., Sudria, A., Bergas, J. and Galceran, S., ”Programmable logic design for an encoder-based velocity sensor in a DSP-controlled motion system”, *Proceedings of the IEEE International Conference on Emerging Technologies and Factory Automation*, vol. 2, 1999, pp 1243-1247.

[6] Briz, F., Cancelas, J.A. and Diez, A., ”Speed measurement using rotary encoders for high performance AC drives”, *Proceedings of the IEEE International Conference on Industrial Electronics, Control and Instrumentation*, vol. 1, no. 5-9, 1994, pp 538-542.

[7] Belanger, P.R., ”Estimation of angular velocity and acceleration from shaft encoder measurements”, *Proceedings of the IEEE International Conference on Robotics and Automation*, vol. 1, 1992, pp 585-592.

[8] Jeffrey B. Burl, *Linear Optimal Control*, Addison Wesley Longman, Inc., 1998, pp 56-57.

[9] Mohinder S. Grewal and Angus P. Andrews, *Kalman Filtering: Theory and Practice*, John Wiley & Sons, Inc., 2001, pp 121.

[10] Luong-Van D. and Katupitiya J., ”An Adaptive Kalman Filter With Quadrature Encoder Quantisation Compensation”, *Proceedings of the IFAC 3rd IFAC Symposium on Mechatronic Systems*, vol. 1, 2004, pp 110-114.